Nonclassical photon-assisted transport in superconducting tunnel junctions

Matthias Hübler [1], Juan Carlos Cuevas [2,3] and Wolfgang Belzig [1]
[1] *Fachbereich Physik, Universität Konstanz, 78457 Konstanz, Germany*
[2] *Departamento de Física Teórica de la Materia Condensada, Universidad Autónoma de Madrid, E-28049 Madrid, Spain*
[3] *Condensed Matter Physics Center (IFIMAC), Universidad Autónoma de Madrid, E-28049 Madrid, Spain*

(Received 30 July 2025; accepted 31 October 2025; published 1 December 2025)

Advances in circuit quantum electrodynamics have enabled the generation of arbitrary nonclassical microwave states, enabling progress in physics. Here, we present a theoretical study of the electrical current in a Josephson tunnel junction interacting with a nonclassical electromagnetic environment. This allows us to generalize classical transport phenomena like photon-assisted tunneling and Shapiro steps to the quantum regime. We predict that the analysis of the supercurrent in such a setup enables the complete reconstruction of quantum states of the electromagnetic environment, something that is not possible with normal tunnel junctions.

DOI: 10.1103/64gy-9vnc

I. INTRODUCTION

Initial investigations of microwave-irradiated Josephson tunnel junctions date back to the early 1960s [1], which, in particular, revealed two textbook phenomena. First, the appearance of microwave-induced steps in the current-voltage characteristics [2], which were interpreted as photon-assisted tunneling of single quasiparticles [3]. Second, the occurrence of Shapiro steps, which consist of additional contributions to the dc current at very specific bias voltages that stem from the phase locking between the ac Josephson current components and the microwave field [4]. These two phenomena illustrated the duality that Josephson junctions can be used as microwave detectors and microwaves can be used to learn about the Josephson effect. With the advent of circuit quantum electrodynamics (circuit QED) in recent years [5,6], and the ability to create nonclassical microwave states almost at will [7], a natural question arises: What novel physical phenomena may result when Josephson tunnel junctions are subjected to nonclassical microwaves?

In fact, the nonclassical microwaves generated by superconducting resonators have already provided insight into the physics of Josephson junctions via microwave spectroscopy of Andreev bound states, see, e.g., Refs. [8,9]. It has also been shown that the coupling of a high impedance microwave resonator to a Josephson tunnel junction can be used for quantum bath engineering [10].

In this work, we address the question above and present a theoretical study of the current-voltage characteristics of Josephson tunnel junctions interacting with nonclassical microwave states. Our main goal is to show that superconducting tunnel junctions can be used as detectors to reveal the nature of nonclassical microwave states beyond the capabilities of normal (nonsuperconducting) tunnel junctions [11]. To be precise, we show how the analysis of the supercurrent and the quasiparticle current flowing through the Josephson junction enables the complete reconstruction of the density matrix of quantum states fabricated with circuit QED setups.

The rest of the manuscript is organized as follows. First, we briefly discuss in Sec. II the general theoretical framework based on the concept of full counting statistics (FCSs) used to compute the tunneling current in a Josephson junction interacting with an arbitrary quantum environment. In Sec. III, we particularize the general formalism to the case of environments consisting of a set of discrete quantum states. Then this formalism is illustrated and applied to two different examples. First, Sec. IV is devoted to the simple example in which the electromagnetic environment consists of a single qubit (or two-level system). Second, in Sec. V we present the results obtained for the case of a single-mode environment and, in particular, we discuss the results for the tunneling current through a Josephson tunnel junction in the case of environmental quantum states of special interest (Fock, coherent, and squeezed states). We summarize the main conclusions of this work in Sec. VI. Finally, the Appendix presents a detailed description of the theoretical framework used to compute the results of this work, as well as some discussions clarifying the connection to previous work in related topics.

II. GENERAL ENVIRONMENT

We investigate how a general electromagnetic environment modifies quantum transport in a superconducting tunnel junction [see Fig. 1(a) for the setup]. The environment imposes a voltage, and thereby a dynamical phase $\hat{\phi}(t)$, across the junction. This phase couples to the tunneling current $\hat{I}$ via the

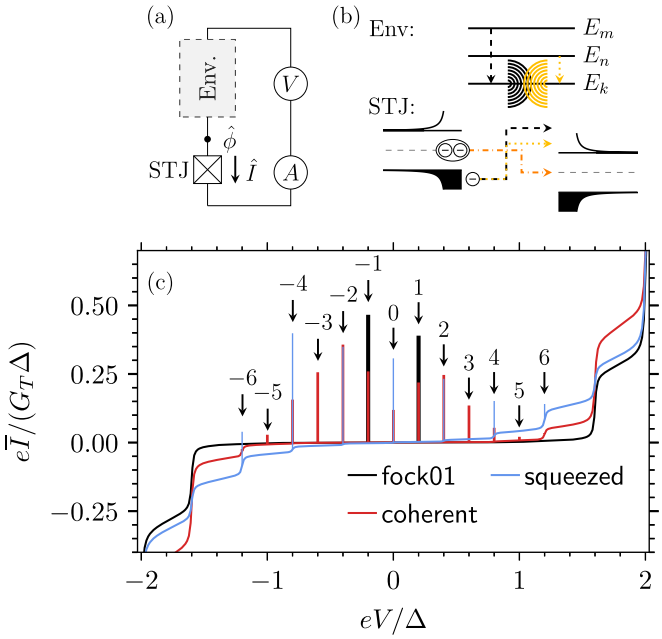

FIG. 1. (a) Superconducting tunnel junction (STJ) interacting with an electromagnetic environment (Env.) that imposes a quantum phase $\hat{\phi}$ on the junction. A dc voltage V is applied and the current-voltage characteristic is investigated. (b) Transitions $E_m \to E_k$ or $E_n \to E_k, \ldots$ between the discrete energy levels of the electromagnetic environment induce quasiparticle transport in the STJ. Interference between a pair of transitions leads to inelastic Cooper pair transport, which manifests as current spikes at $eV = (E_m - E_n)/2$ in the dc current. (c) dc current as a function of the voltage for an STJ at zero temperature, coupled to an LC-resonator with frequency $\hbar\omega_0 = 0.4\Delta$ and coupling strength $g = 1/2$. The oscillator is in the states defined in Eqs. (12), where $|\xi| = |\alpha| = 1$, and the phases are arbitrary. The spikes represent the amplitude of the Cooper pair current-phase relation (14c), while the background corresponds to the quasiparticle current (13a). Spikes appear at $eV = j\hbar\omega_0/2$ (indicated by the arrows), whereas steps occur at $eV = 2\Delta + l\hbar\omega_0$, with $j, l \in \mathbb{Z}$.

interaction term $\hat{H}_{\rm int}(t) = (\hbar/e)\,\hat{\phi}(t)\hat{I}$, where $\hbar$ is the reduced Planck's constant and e is the elementary charge. For example, a constant voltage bias V induces the phase $\hat{\phi}(t) = \varphi_{\rm dc}(t) = eV(t - t_s)/\hbar + \phi_0/2$, with $\phi_0/2$ the phase at the initial time t_s. Photon-assisted tunneling is described by an additional phase $\varphi(t) = a\sin(s\omega_0(t - t_s))$, with a the strength of the classical drive, and ω_0 the driving frequency [1,3]. A quantum environment introduces a phase operator $\hat{\varphi}$, whose dynamics is governed by an environmental Hamiltonian $\hat{H}_{\rm env}$. In the interaction picture, this phase evolves as $\hat{\varphi}(t) = \exp(i\hat{H}_{\rm env}(t - t_s))\hat{\varphi}\exp(-i\hat{H}_{\rm env}(t - t_s))$ leading to a total phase across the junction given by $\hat{\phi}(t) = \hat{\varphi}(t) + \varphi_{\rm dc}(t)$.

Our goal is the analysis of the tunnel current in a superconducting junction arising from both a voltage bias and an arbitrary quantum electromagnetic environment [see Fig. 1(a)]. For this purpose, we employ the Keldysh formalism [12] to compute the cumulant-generating functional (CGF) of the hybrid system to the lowest order in the tunnel conductance $G_{\rm T}$. To improve the readability of the paper, the relevant technical details are discussed in depth in the Appendix. This formalism has been used to treat mesoscopic conductors under arbitrary classical drives [13,14], as well as electromagnetic environments in equilibrium [15–17]. In principle, the current, noise, and higher-order cumulants can be obtained from the CGF. We focus here on the tunnel current, as it already captures a broad range of physical effects.

As shown in Appendix Sec. A 6, the tunnel current comprises quasiparticle (QP) and Cooper pair (CP) transport, and takes the form

$$I(t) = I_{\rm QP}(t) + I_{\rm CP}(t)$$
$$= \sum_{\nu=\pm} \nu \int_{-\infty}^{\infty} dE\, P^{\nu}(t, E)\Gamma_{\rm QP}(E) \tag{1a}$$
$$+ \sum_{\nu=\pm} \nu \int_{-\infty}^{\infty} dE\, C^{\nu}(t, E)\Gamma_{\rm CP}(E). \tag{1b}$$

Both contributions depend on the tunneling rate of the isolated junction, which are given by

$$\Gamma_{\rm QP}(E) = \frac{G_{\rm T}}{e}\int_{-\infty}^{\infty} d\epsilon\, \varrho_1(\epsilon - E)\varrho_2(\epsilon)[1 - f(\epsilon - E)]f(\epsilon) \tag{2a}$$

$$\Gamma_{\rm CP}(E) = \frac{G_{\rm T}}{e}\int_{-\infty}^{\infty} d\epsilon\, \varsigma_1(\epsilon - E)\varsigma_2(\epsilon)[1 - f(\epsilon - E)]f(\epsilon), \tag{2b}$$

where

$$\varrho_p(E) = \mathrm{Re}\left(\frac{-i(E + i\eta)}{\sqrt{\Delta_j^2 - (E + i\eta)^2}}\right) \tag{2c}$$

is the normalized quasiparticle density of states,

$$\varsigma_p(E) = \mathrm{Re}\left(\frac{i\Delta_j}{\sqrt{\Delta_j^2 - (E + i\eta)^2}}\right) \tag{2d}$$

is the normalized pair density with $\eta \ll 1$ the broadening parameter, $\Delta_p \equiv \Delta$ is the superconducting gap of terminal $p = 1, 2$, and $f(E) = [1 + \exp(E/(k_{\rm B}T))]^{-1}$ is the Fermi-distribution at thermal energy $k_{\rm B}T$. Here, the terminals are assumed to be s-wave superconductors. The $\nu = +$ terms in Eqs. (1a) and (1b) describe transport from terminal 2 to terminal 1, while the $\nu = -$ terms describe transport in the opposite direction. The environment influences the transport via the generalized P functions [11]

$$P^{\nu}(t, E) = \int_{-\infty}^{\infty} d\tau\, \mathrm{Im}\left(e^{iE\tau/\hbar}G^{\nu+}_{\rm env}(t, \tau)\right) \tag{3a}$$

and C functions

$$C^{\nu}(t, E) = \int_{-\infty}^{\infty} d\tau\, \mathrm{Im}\left(e^{iE\tau/\hbar}G^{\nu-}_{\rm env}(t, \tau)\right), \tag{3b}$$

which depend on the environmental correlator

$$G^{\nu\mu}_{\rm env}(t, \tau) = \frac{i}{\pi\hbar}\Theta(\tau)\langle e^{i\mu\nu\hat{\phi}(t)}e^{-i\nu\hat{\phi}(t-\tau)}\rangle. \tag{3c}$$

The correlators contain the translation operator $\hat{\mathcal{T}} \equiv e^{-i\hat{\phi}(t)}$, which shifts the junction's charge by one elementary charge e [18]. In the P functions ($\sim\langle\hat{\mathcal{T}}^{\dagger}(t)\hat{\mathcal{T}}(t-\tau)\rangle$), an elementary charge is removed from the junction at time $t-\tau$ and restored at t. In contrast, the correlators in the C-function ($\sim\langle\hat{\mathcal{T}}(t)\hat{\mathcal{T}}(t-\tau)\rangle$) correspond to removing two elementary charges from the junction, one at $t-\tau$ and the other at t.

The structure of the quasiparticle current $I_{\mathrm{QP}}(t)$ is identical to that found in a normal-metal tunnel junction coupled to an arbitrary electromagnetic environment [11]. The only difference is that the quasiparticle rates involve the superconducting rather than the normal-metal density of states. The P functions in Eq. (3a) coincide with that of the normal-metal case [11] and reduce to the known result from dynamical Coulomb blockade theory for an environment in equilibrium [18–20]. The key difference between a quantum and a classical environment is that phase operators at different times do not commute, leading to distinct P functions ($\nu=\pm$) for charge transport from terminal 1 to 2 versus from 2 to 1. If the phase operator commutes at all times, the symmetry $P^{-}(t,E)=P^{+}(t,-E)$ is recovered. This symmetry ensures that the current depends directly on the bare current, $I^{0}_{\mathrm{QP}}(E)=\Gamma_{\mathrm{QP}}(-E)-\Gamma_{\mathrm{QP}}(E)$, as is the case in photon-assisted tunneling [1,3,4]. In a normal-metal junction, this noncommutativity leads to a nonlinear I-V characteristic, as opposed to the linear behavior predicted by photon-assisted tunneling, which is attributed to the zero-point fluctuations of the field [11].

The Cooper pair current $I_{\mathrm{CP}}(t)$ has a similar structure, with the density of states replaced by the pair density, but with the exponents in the environmental correlators carrying the same sign. This sign difference profoundly affects the system's behavior: it induces dependence on the superconducting phase ϕ_0 and on $2eVt/\hbar$, which are the basis for the dc and ac Josephson effects as well as the Shapiro effect. For example, the standard dc Josephson effect is recovered when the phase is constant ($\hat{\phi}(t)=\phi_0/2$), resulting in a sinusoidal current-phase relation. A dc bias induces a linear time-dependence of the phase ($\hat{\phi}(t)=eVt/\hbar$), leading to an oscillating Cooper pair current at the Josephson frequency, as can be derived from Eqs. (3), see Appendix Sec. A 7 for details.

III. DISCRETE SPECTRUM

We focus now on a broad class of environments composed of discrete modes. This class is encountered in circuit QED systems [5], where the environment may consist of an LC resonator, an artificial atom, a superconducting qubit, etc. The environmental Hamiltonian $\hat{H}_{\mathrm{env}}$ has a discrete spectrum, with eigenenergies E_n and eigenstates $|E_n\rangle$. The phase $\hat{\varphi}(t)$ evolves according to the unitary operator $\hat{U}(t,t_s)$, which takes the spectral form $\hat{U}(t,t_s)=\sum_n \exp(-iE_n(t-t_s))\,|E_n\rangle\langle E_n|$, where the sum runs over all eigenstates. We consider the electromagnetic environment to be initialized in a general quantum state, described by the density matrix $\hat{\rho}$. The environmental correlator reduces to

$$\langle e^{-i\nu\hat{\varphi}(t)}e^{-i\nu'\hat{\varphi}(t-\tau)}\rangle = \sum_{n,m,k}\langle\hat{L}_{mk}\hat{L}_{kn}\rangle A^{\nu}_{mk}A^{\nu'}_{kn} \times e^{-i(E_k-E_n)\tau/\hbar - i(E_n-E_m)t/\hbar}, \tag{4}$$

with the ladder operator $\hat{L}_{kn}=|E_k\rangle\langle E_n|$ corresponding to the transition $E_n\to E_k$, and the transition amplitude $A^{\nu}_{kn}=\langle E_k|\exp(-i\nu\hat{\varphi})\,|E_n\rangle$. The operator $\exp(-i\nu\hat{\varphi})$ acts as a translation operator for the charge operator $\hat{Q}$, which is canonically conjugate to the phase $\hat{\varphi}$, shifting the charge in the environment by one elementary unit [18].

The current $I(t)$ oscillates in time, and we focus on its dc component, given by the long-time average $\bar{I}=\lim_{\tilde{T}\to\infty}(1/\tilde{T})\int_{-\tilde{T}/2}^{\tilde{T}/2} I(t)dt$. The quasiparticle current is a superposition of oscillations at transition frequencies between the states, and the time-averaged current is given by

$$\bar{I}_{\mathrm{QP}}=\sum_{\nu=\pm}\nu\sum_{n,k}\gamma^{\nu}[k,n]\Gamma_{\mathrm{QP}}(E_k-E_n-\nu eV), \tag{5a}$$

where

$$\gamma^{\nu}[k,n]=|A^{\nu}_{kn}|^2\mathrm{Tr}\{\hat{L}_{kn}\hat{\rho}\hat{L}^{\dagger}_{kn}\}=|A^{\nu}_{kn}|^2\rho_{nn}. \tag{5b}$$

Here, ρ_{nn} are the diagonal entries of the density matrix in the energy basis and $\mathrm{Tr}\{\cdot\}$ represents the trace. The transition rate $\gamma^{\nu}[k,n]$ from state E_n to state E_k involves the transition probability $|A^{\nu}_{kn}|^2$ induced by the charge transport and the occupation probability of the initial state ρ_{nn}. The transition rates satisfy the normalization condition $\sum_{k,n}\gamma^{\nu}[k,n]=1$, reflecting the conservation of probability. Figure 1(b) illustrates quasiparticle transport processes.

Due to the ac Josephson effect, the oscillations in the Cooper pair current are shifted by the Josephson frequency $\omega_{\mathrm{J}}=2eV/\hbar$, such that the current becomes a superposition of oscillatory components at frequencies $\omega_{\mathrm{J}}+(E_n-E_m)/\hbar$. The time-averaged Cooper pair current is given by

$$\bar{I}_{\mathrm{CP}}=\sum_{m,n}\delta_{eV,(E_m-E_n)/2}\,\bar{I}^{\mathrm{CP}}_{mn}, \tag{6a}$$

where $\delta_{x,y}$ equals one for $x=y$ and zero otherwise. Therefore, the transport of Cooper pairs results in spikes in the dc I-V characteristics, occurring when the applied voltage satisfies the resonance condition $eV=(E_m-E_n)/2$. For an overview, Fig. 1(c) shows the spike structure due to Cooper pair transport, along with the steplike quasiparticle current resulting from an LC-resonator used as the environment. Each pair of states $|E_m\rangle$, $|E_n\rangle$ contributes

$$\bar{I}^{\mathrm{CP}}_{mn}=\sum_{k}\Gamma_{\mathrm{S}}\left(E_k-\frac{E_m+E_n}{2}\right)\mathrm{Im}(e^{i\phi_0}C_{nkm}), \tag{6b}$$

with

$$\Gamma_{\mathrm{S}}(E)=2\,\mathrm{P.V.}\int_{-\infty}^{\infty}d\epsilon\,\frac{\Gamma_{\mathrm{CP}}(\epsilon)}{\pi(\epsilon-E)} \tag{6c}$$

$$C_{nkm}=(A^{+}_{kn})^{*}A^{-}_{km}\mathrm{Tr}\{\hat{L}_{km}\hat{\rho}\hat{L}^{\dagger}_{kn}\} =(A^{+}_{kn})^{*}A^{-}_{km}\rho_{mn}, \tag{6d}$$

where P.V. denotes principal value. The rate $\Gamma_{\mathrm{S}}(eV)$ is related to the ac Josephson current $I_{c,1}(V)\sin(\phi_0+\omega_{\mathrm{J}}t)$ by [1]

$$I_{c,1}(V)=[\Gamma_{\mathrm{S}}(eV)+\Gamma_{\mathrm{S}}(-eV)]/2. \tag{7}$$

The factor C_{nkm} incorporates the effect of the environment and contains the transition amplitudes A^{+}_{kn} and A^{-}_{km}. We interpret this factor as an interference contribution between the transitions E_m to E_k and E_n to E_k, with an initial coherence

ρ_{mn} being necessary to generate interference between the transitions; see Fig. 1(b). Degenerate energy splittings among multiple levels lead to their collective contribution to a single spike in the I-V characteristics. If all transition energies are distinct, the spike height is directly proportional to the coherences ϱ_{mn} of the environmental density matrix, enabling their direct extraction.

The physics at play here is closely related to the Shapiro effect that occurs under a harmonic current drive [1,4]. There, voltage plateaus emerge at multiples of half the driving frequency, manifesting as current spikes in the voltage-source model [1]. Here, the spikes occur at the transition energies of the environment and need not be regularly spaced.

Note that a system in equilibrium, or in an incoherent superposition of energy eigenstates, does not exhibit spikes at finite voltage. Interestingly, a modified supercurrent $\bar{I}^{\mathrm{CP}} = \sum_{n,k} \Gamma_S(E_k - E_n)\,\mathrm{Im}(e^{i\phi_0} C_{nkn})$ arises even in equilibrium. This is in contrast to predictions from standard dynamical Coulomb blockade theory [18], where the supercurrent vanishes and the first nonzero contribution to the Cooper pair current is second order in the tunnel conductance. In Ref. [18], the Cooper pair condensate was modeled using the Josephson Hamiltonian. The microscopic analysis [19] shows that the supercurrent survives for environments in which the real part of the impedance vanishes as $\mathcal{O}(\omega^2)$ or faster as $\omega \to 0$. A set of discrete modes satisfies this scaling behavior and the supercurrent remains finite.

IV. EXAMPLE 1: QUBIT

To illustrate the physics, we consider a superconducting qubit (e.g., a charge qubit or a transmon [5]) acting as the electromagnetic environment. Working within a two-level truncation, the environmental Hamiltonian is $\hat{H}_{\mathrm{env}} = -\hbar\omega_q \hat{\sigma}_3/2$, where $\hbar\omega_q$ is the level spacing and $\hat{\sigma}_3$ the third Pauli matrix. Accordingly, the superconducting tunnel junction couples to the phase operator $\hat{\varphi} = \varphi_{\mathrm{zpf}}\hat{\sigma}_1$, where $\varphi_{\mathrm{zpf}} = (2E_{\mathrm{c}}/E_{\mathrm{J}})^{1/4}$ denotes the zero-point phase fluctuations, E_{C} and E_{J} are the charging and Josephson energies, respectively, and $\hat{\sigma}_1$ the first Pauli matrix [5]. The state of the qubit is encoded in the density matrix

$$\hat{\rho} = \begin{pmatrix} \rho_{00} & \rho_{01} \\ \rho_{10} & \rho_{11} \end{pmatrix}, \tag{8}$$

with elements ρ_{jk} ($j,k \in \{0,1\}$) satisfying $\rho_{00} + \rho_{11} = 1$ and $\rho_{10} = \rho_{01}^*$.

The dc quasiparticle current through the superconducting junction is given by Eq. (5a) and reduces to

$$\begin{aligned} \bar{I}_{\mathrm{QP}} = {} & \bar{I}^0_{\mathrm{QP}}(eV)\cos^2(\varphi_{\mathrm{zpf}}) \\ & + \rho_{00}\sin^2(\varphi_{\mathrm{zpf}}) \sum_{\nu=\pm} \nu\Gamma_{\mathrm{QP}}(\hbar\omega_q - \nu eV) \\ & + \rho_{11}\sin^2(\varphi_{\mathrm{zpf}}) \sum_{\nu=\pm} \nu\Gamma_{\mathrm{QP}}(-\hbar\omega_q - \nu eV), \end{aligned} \tag{9}$$

where $\bar{I}^0_{\mathrm{QP}}(eV)$ refers to the bare current-voltage characteristics, which exhibit an onset of quasiparticle current at $|eV| = 2\Delta$. Transitions from the excited state $|1\rangle$ to the ground state $|0\rangle$ give rise to subgap transport that sets in at $eV = 2\Delta - \hbar\omega_q, -2\Delta + \hbar\omega_q$. Conversely, transitions $|0\rangle \to |1\rangle$ appear at $eV = 2\Delta + \hbar\omega_q, -2\Delta - \hbar\omega_q$. Therefore, the quasiparticle current features at most three steplike onsets: a subgap step that occurs when the excited state is populated ($\rho_{11} \neq 0$) and an above-gap step that occurs when the ground state is populated ($\rho_{00} \neq 0$). Figure 2 shows the quasiparticle current for different qubit states. Therefore, measurement of the quasiparticle current enables extraction of the diagonal elements of the qubit density matrix.

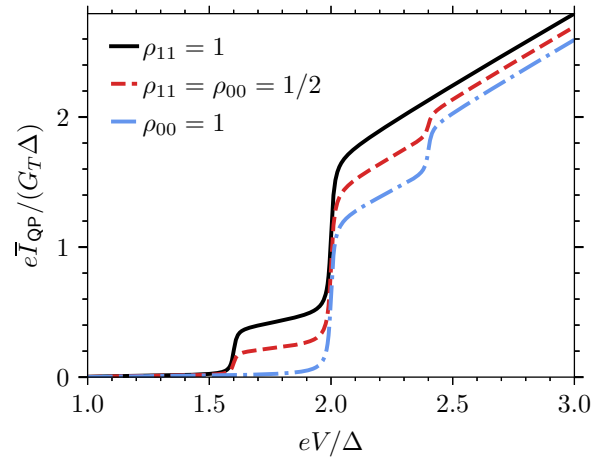

FIG. 2. Quasiparticle current $\bar{I}_{\mathrm{QP}}$ for an environmental qubit prepared in the ground state ($\rho_{00} = 1$), the excited state ($\rho_{11} = 1$), and an equal mixture ($\rho_{00} = \rho_{11} = 1/2$). The zero-point fluctuations are $\varphi_{\mathrm{zpf}} = 0.5$, the qubit frequency is $\hbar\omega_q = 0.4\Delta$, and the tunnel rate 2(a) is evaluated at zero temperature with a broadening parameter $\eta = 5 \times 10^{-3}$.

On the other hand, Cooper pair transport leads to current spikes at $eV = 0$ ($\bar{I}^{\mathrm{CP}}_0$), $eV = \hbar\omega_q/2$ ($\bar{I}^{\mathrm{CP}}_+$), and $eV = -\hbar\omega_q/2$ ($\bar{I}^{\mathrm{CP}}_-$). The zero-bias current corresponds to a modified supercurrent and takes the form

$$\bar{I}^{\mathrm{CP}}_0 = \tilde{I}_c \sin(\phi_0), \tag{10a}$$

with an effective critical current

$$\begin{aligned} \tilde{I}_c = {} & I_c\cos^2(\varphi_{\mathrm{zpf}}) - \rho_{00}\Gamma_{\mathrm{S}}(\hbar\omega_q/2)\sin^2(\varphi_{\mathrm{zpf}}) \\ & + \rho_{11}\Gamma_{\mathrm{S}}(-\hbar\omega_q/2)\sin^2(\varphi_{\mathrm{zpf}}), \end{aligned} \tag{10b}$$

where I_c is the critical current without environment. In the limit $\hbar\omega_q \ll \Delta$, the effective critical current reduces to $\tilde{I}_c \approx I_c\cos(2\varphi_{\mathrm{zpf}}) \in [-I_c, I_c]$ and is therefore independent of the qubit state, depending only on φ_{zpf}. The frequency dependence is governed by the rate Γ_{S} in Eq. (6c), which exhibits the Riedel singularity shown in Fig. 3. Transitions between the qubit levels ($|0\rangle \leftrightarrow |1\rangle$) reduce the effective critical current. It can become negative, reflecting a phase shift of π and, due to the Riedel peak, can even be smaller than $-I_c$. Figure 4 shows the effective critical current $\tilde{I}_c$ for different zero-point fluctuations and qubit frequencies. The global minimum $\min_{\varphi_{\mathrm{zpf}},\omega_q,\hat{\rho}} \tilde{I}_c$ is achieved for $\rho_{11} = 1$, $\varphi_{\mathrm{zpf}} = \pi/2$, $\hbar\omega_q = 4\Delta$. For the ground state $\rho_{00} = 1$, the minimum equals $-I_c$ at $\varphi_{\mathrm{zpf}} = \pi/2$ and $\hbar\omega_q = 0$.

The finite-bias spikes have peak heights

$$\bar{I}^{\mathrm{CP}}_{\pm} = |\rho_{10}| I_{c,1}(\hbar\omega_q/2)\sin(2\varphi_{\mathrm{zpf}})\cos(\phi_0 \pm \vartheta_{10}), \tag{11}$$

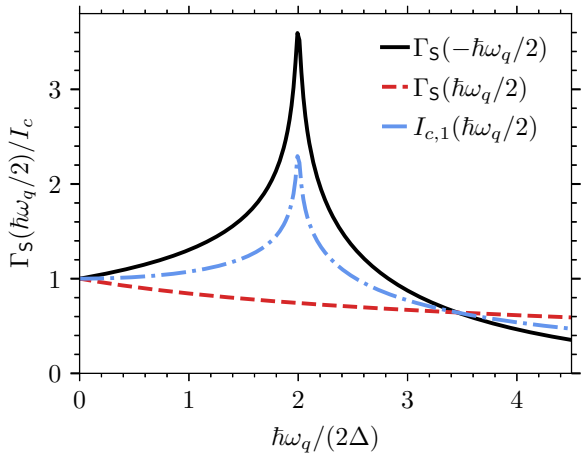

FIG. 3. Rate Γ_S and amplitude of the ac Josephson current $I_{c,1}$ that enter the Cooper-pair transport. Parameter: zero temperature; broadening parameter $\eta = 5 \times 10^{-3}$.

where $\rho_{10} = |\rho_{10}|e^{i\vartheta_{10}}$. Here $I_{c,1}(\hbar\omega_q/2)$ is the voltage-dependent current amplitude known from the Shapiro effect (see Eq. (A27b) and Ref. [1]). Figure 3 displays the current amplitude $I_{c,1}$, which sets the frequency dependence of the spikes. Overall, the two finite-bias current spikes provide information about the qubit coherence $|\rho_{10}|$.

V. EXAMPLE 2: QUANTUM HARMONIC OSCILLATOR

Let us turn now to the case of a single electromagnetic mode modeled as a quantized LC circuit. The flux $\hat{\Phi} = \hbar\hat{\varphi}/e$ through the inductor is related to the phase operator $\hat{\varphi} = -i\sqrt{g}(\hat{a} - \hat{a}^\dagger)$, with $g = \pi Z_{LC}/R_K$ the strength of the zero-point voltage fluctuations, determined by the impedance of the resonator $Z_{LC} = \sqrt{L/C}$ and the resistance quantum $R_K = 2\pi\hbar/e^2$, and $\hat{a}/\hat{a}^\dagger$ the annihilation/creation operator of the mode. The oscillator has eigenenergies $E_n = \hbar\omega_0(n + 1/2)$ and Fock states $|n\rangle$, with transition energies $E_{n+l} - E_n = l\hbar\omega_0, l \in \mathbb{Z}$ between the states, where $\omega_0 = 1/\sqrt{LC}$ is the resonance frequency. To explore how different quantum states influence the transport, we prepare the oscillator in either a Fock superposition

$$|\Psi_{01}\rangle = \frac{|0\rangle + \exp(i\theta_1)\,|1\rangle}{\sqrt{2}}, \tag{12a}$$

a squeezed vacuum state

$$|\xi\rangle = \sum_{n=0}^{\infty}(-1)^n \frac{\sqrt{(2n!)}}{2^n n!}\exp(in\theta_2)\frac{(\tanh(|\xi|))^n}{\sqrt{\cosh(|\xi|)}}\,|2n\rangle\,, \tag{12b}$$

or a coherent state

$$|\alpha\rangle = \exp\left(-\frac{|\alpha|^2}{2}\right)\sum_{n=0}^{\infty}\frac{|\alpha|^n e^{in\theta_3}}{\sqrt{n!}}\,|n\rangle\,. \tag{12c}$$

The squeezed state is controlled by the squeezing amplitude $|\xi|$, which characterizes the degree of squeezing, while the coherent state depends on $|\alpha|$, which determines the amplitude of the oscillations. All states can carry an associated phase θ_s $(s = 1, 2, 3)$. By simple inspection, we can infer from Eq. (6d) and the properties of the states which Cooper pair current spikes may appear in the I-V characteristics. Since $|\psi_{01}\rangle$ only has nonzero coherences on the first off-diagonals of the density matrix, spikes only appear at $eV = -\hbar\omega_0/2, 0, \hbar\omega_0/2$. A squeezed vacuum state possesses nonzero entries only for even occupation numbers, so no peaks appear at $eV = j\hbar\omega_0/2$, with j odd. In contrast, a coherent state can have spikes at all $j \in \mathbb{Z}$ due to its nonzero coherences across all Fock states. The distinct coherence structures of these states are directly reflected in the Cooper pair transport [see Fig. 1(c)].

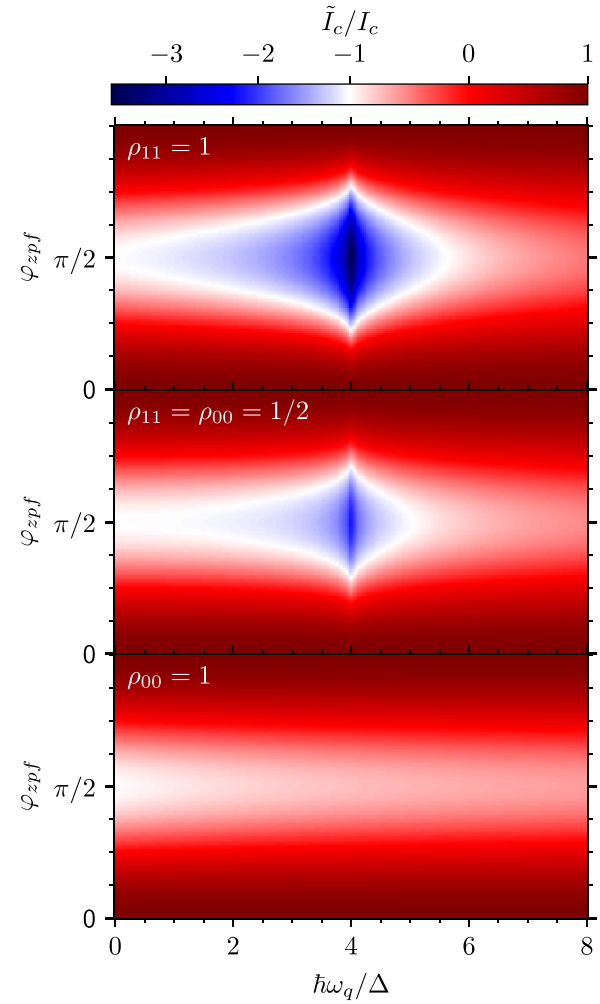

FIG. 4. Effective critical current $\tilde{I}_c$ for an environmental qubit prepared in the ground state ($\rho_{00} = 1$), the excited state ($\rho_{11} = 1$), and an equal mixture ($\rho_{00} = \rho_{11} = 1/2$). The effective critical current can become negative and, in magnitude, exceed the (no-environment) critical current due to the Riedel peak. Parameter: zero temperature; broadening parameter $\eta = 5 \times 10^{-3}$.

The background current in Fig. 1(c) arises from quasiparticle transport and is described by

$$\bar{I}_{QP} = \sum_{l=-\infty}^{\infty} p[l]\sum_{\nu=\pm}\nu\Gamma_{QP}(l\hbar\omega_0 - \nu eV), \tag{13a}$$

where the quasiparticles exchange l energy quanta with the environment, with probability

$$p[l] = \sum_{n=0}^{\infty}\Theta(n+l)|A^-_{n+ln}|^2\rho_{nn}, \tag{13b}$$

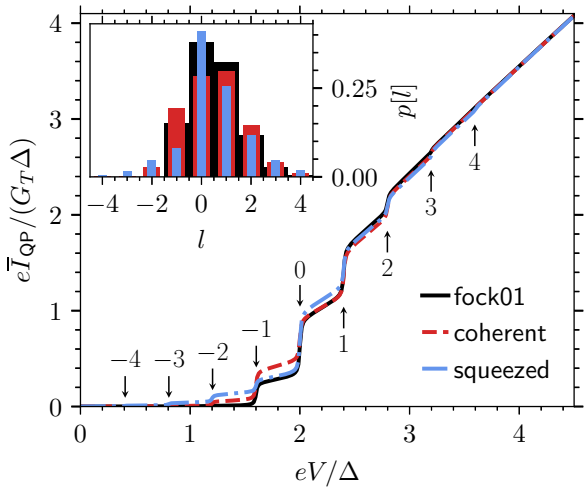

FIG. 5. Quasiparticle current $\bar{I}_{QP}$ for the three different environmental states given in Eqs. (12). The inset displays the probability $p[l]$ for exchanging l energy quanta with the environment, while the arrows indicate the positions $2\Delta + l\hbar\omega_0$, where the lth energy exchange begins to contribute to the current. The parameters controlling the states are set to $|\xi| = |\alpha| = 1$, $\theta_s \in \mathbb{R}$. The oscillator is characterized by $\hbar\omega_0 = 0.4\Delta$, $g = 1/2$, and the tunnel rate (2a) is evaluated at zero temperature with a broadening parameter $\eta = 5 \times 10^{-3}$.

determined by the transition amplitudes

$$A^{v}_{n+ln} = e^{-g/2} \begin{cases} \sqrt{\frac{n!}{(n+l)!}} (vg)^{l/2} L^{l}_{n}(g) & l \geqslant 0 \\ \sqrt{\frac{(n+l)!}{n!}} (-vg)^{-l/2} L^{-l}_{n+l}(g) & l < 0. \end{cases} \tag{13c}$$

Here, $L^{l}_{n}(x)$ are generalized Laguerre polynomials.

Figure 5 shows the quasiparticle current for the three environmental states in Eqs. (12). Due to the superconducting energy gap, the quasiparticle rate $\Gamma_{QP}(E)$ becomes nonzero only for $E \leqslant -2\Delta$. Therefore, the processes involving the exchange of l energy quanta with the resonator set in successively at $2\Delta + l\hbar\omega_0$, where the exchange probability $p[l]$ determines the height of the step. For example, the Fock superposition can emit at most one excitation, implying $p[l] = 0$ for $l < -1$. As a result, the first step appears at $eV = 2\Delta - \hbar\omega_0$, whereas for the squeezed state, the first step occurs at $2\Delta - 4\hbar\omega_0$. The successive appearance of the steps enables direct extraction of the exchange probability $p[l]$ from the quasiparticle current. In contrast, for normal-conducting junctions, determining the exchange probability requires both the average current and current noise [11]. As proposed by Souquet *et al.* [11], the exchange probability can serve as a diagnostic tool to distinguish classical from nonclassical states.

Cooper pair transport occurs at $eV = j\hbar\omega_0/2$, $j \in \mathbb{Z}$, and the height of the resulting current spike is given by

$$\bar{I}^{CP}_{j} = \sum_{l=-\infty}^{\infty} \Gamma_S([l - j/2]\hbar\omega_0)\, \mathrm{Im}(e^{i\phi_0} \mathcal{C}[l, j]), \tag{14a}$$

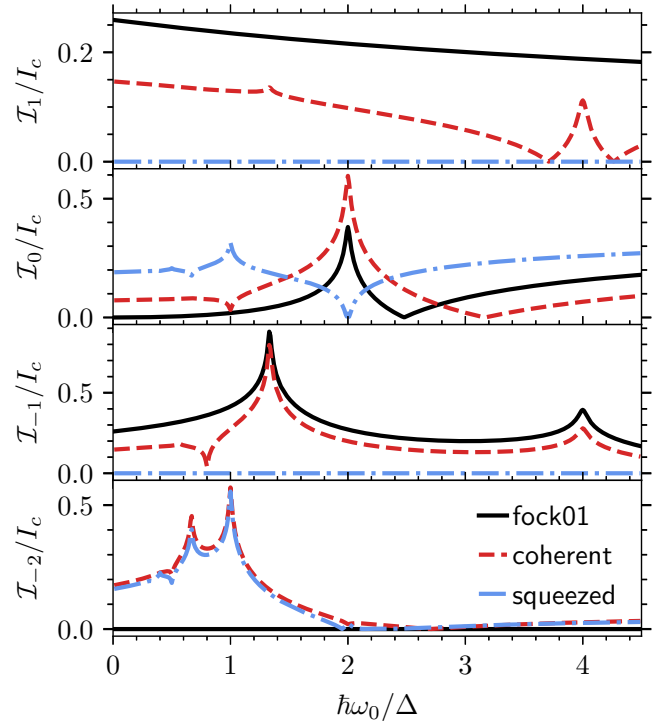

FIG. 6. Cooper pair current amplitudes $\mathcal{I}_j$ [see Eq. (14c)] as a function of frequency for the three different environmental states defined in Eqs. (12). The amplitude is normalized to the critical current I_c of the junction in the absence of an environment, and the tunnel rate in Eq. (2b) is calculated at zero temperature with broadening $\eta = 5 \times 10^{-3}$. The state parameters are set to $|\xi| = |\alpha| = 1$ with arbitrary phases $\theta_s \in \mathbb{R}$, while the coupling is $g = 1/2$.

where

$$\mathcal{C}[l, j] = \sum_{n=0}^{\infty} \Theta(n + l)\Theta(n + j) A^{-}_{nn+l} A^{-}_{nn+j} \rho_{n+jn}. \tag{14b}$$

This expression reduces to a current-phase relation

$$\bar{I}^{CP}_{j} = \mathcal{I}_j \sin(\phi_0 - \vartheta_j), \tag{14c}$$

with the amplitude $\mathcal{I}_j$ and phase shift ϑ_j depending on the environmental state, the coupling strength $\sqrt{g}$, and the resonator frequency ω_0. The jth spike is sensitive to the jth diagonal of the density matrix ρ_{n+jn}. A φ_0 junction cannot be realized in this case, as the modified supercurrent $\bar{I}^{CP}_{0}$ depends only on the diagonal elements of the density matrix, which are real. This leads to $\vartheta_0 = 0$, implying a purely sinusoidal current-phase relation.

Figure 6 shows the frequency dependence of the Cooper pair current amplitudes. The frequency dependence exhibits sharp features at specific frequencies, which are related to Riedel peaks, which are singularities at $|eV| = 2\Delta$ in the ac Josephson current amplitude [1]. Here, the superconducting rate is related to the ac Josephson current amplitude through Eq. (7). In contrast, the rate is asymmetric in energy and exhibits a Riedel peak only at $E = -2\Delta$; see Appendix Sec. A 7. Hence, the frequency dependence of the amplitude $\mathcal{I}_j$ consists of replicas of the Riedel peak at $\hbar\omega_0 = -4\Delta/(2l - j)$, weighted by the interference factors $\mathcal{C}[l, j]$. Kinks at $\mathcal{I}_j = 0$

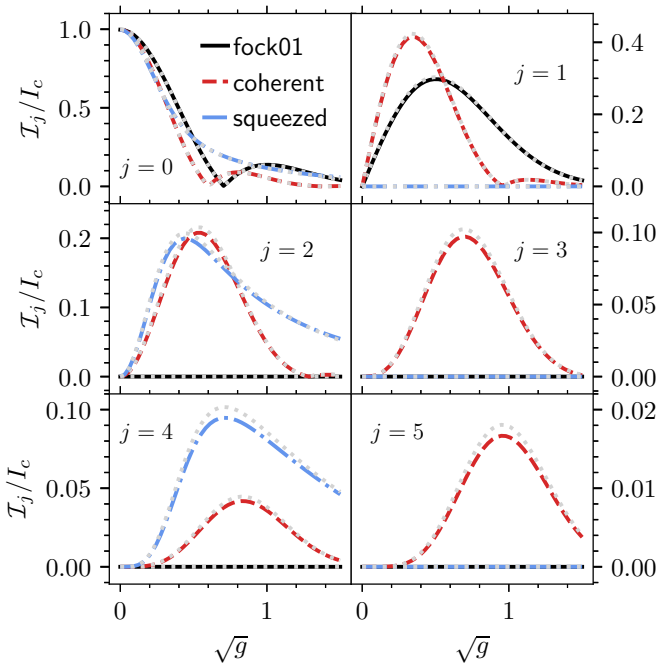

FIG. 7. Cooper pair current amplitudes $\mathcal{I}_j$ [see Eq. (14c)] as a function of the coupling strength $\sqrt{g}$ for $\hbar\omega_0 = 0.1\Delta$. The bare critical current I_c is used to normalize the amplitudes, and the tunnel rate in Eq. (2b) is calculated at zero temperature with broadening $\eta = 5 \times 10^{-3}$. The amplitudes are evaluated for the three environmental states defined in Eqs. (12), where each $\mathcal{I}_j$ probes the jth diagonal of the corresponding density matrix. The state parameters are given by $|\xi| = |\alpha| = 1$ with arbitrary phases $\theta_s \in \mathbb{R}$. The gray dashed lines indicate the zero-frequency limit, which depends solely on the transition amplitudes $\tilde{A}^-_{nn+j}$ and the density matrix elements ρ_{n+jn}.

indicate a sign change of the spike and arise from taking the absolute value, $\mathcal{I}_j = |\bar{I}^{\mathrm{CP}}_j|$.

Figure 7 shows the coupling dependence of the amplitudes $\mathcal{I}_j$ for $\hbar\omega_0 = 0.1\Delta$ and compares it to the zero-frequency limit (gray dashed lines). Varying the coupling strength modifies the transition amplitudes and, consequently, the interference factor (14b). The interference factor satisfies the identity $\sum_{l,j} \mathcal{C}[l, j] = \langle e^{2\sqrt{g}(\hat{a}-\hat{a}^\dagger)}\rangle \equiv M[2\sqrt{g}]$, which corresponds to the moment-generating function of the quadrature $\hat{a} - \hat{a}^\dagger$ evaluated at $2\sqrt{g}$. As $\omega_0 \to 0$, the total Cooper pair current reduces to an expression involving the moment-generating function, $\sum_j \bar{I}^{\mathrm{CP}}_j = I_c \,\mathrm{Im}(e^{i\phi_0} M[2\sqrt{g}])$, where $I_c = \Gamma_S(0)$ is the critical current of the uncoupled junction. The individual amplitudes take the form $\lim_{\omega_0\to 0} \mathcal{I}_j = I_c |\sum_n \Theta(n + j)\tilde{A}^-_{nn+j}\rho_{n+jn}|$, with a rescaled transition amplitude $\tilde{A}^-_{nn+j} = \langle n| \exp(2i\hat{\varphi}) |n + j\rangle$. Thus, the coupling dependence serves as a sensitive indicator of the environmental state.

VI. CONCLUSIONS

We have shown that the coupling between a nonclassical electromagnetic environment and a Josephson tunnel junction gives rise to a very rich phenomenology in the current-voltage characteristics. In particular, we have illustrated how a superconducting tunnel junction can be used to completely characterize the nature of quantum states generated with circuit-QED setups, something that is not possible with normal tunnel junctions. Moreover, with the theoretical framework used here, the analysis of the transport characteristics can be straightforwardly extended to the study of higher-order cumulants like shot noise.

ACKNOWLEDGMENTS

We sincerely thank B. Reulet and D. Christian Ohnmacht for helpful discussions. This research was supported by the Deutsche Forschungsgemeinschaft (DFG; German Research Foundation) via SFB 1432 (Project No. 425217212), which, in particular, sponsored the stay of J.C.C. at the University of Konstanz as a Mercator Fellow.

DATA AVAILABILITY

The data that support the findings of this article are not publicly available upon publication because it is not technically feasible and/or the cost of preparing, depositing, and hosting the data would be prohibitive within the terms of this research project. The data are available from the authors upon reasonable request.

APPENDIX: THEORETICAL FORMALISM

In this Appendix, we present a detailed description of the theoretical formalism employed to obtain the results of the main text.

1. Hamiltonian

Our objective is to analyze the impact of an arbitrary electromagnetic environment on the current through a superconducting tunnel junction. In the absence of an environment, quantum transport in the tunnel junction is governed by the Hamiltonian $\hat{H}_{\mathrm{cond}}$ [18,21–23]. We model the coupling between the junction and the environment via the interaction Hamiltonian

$$\hat{H}_{\mathrm{int}} = \frac{\hbar}{e}\hat{\phi}(t)\hat{I}, \tag{A1a}$$

where $\hat{I}$ denotes the junction's current operator, $\hat{\phi}(t)$ represents the phase operator associated with the electromagnetic environment, and e corresponds to the elementary charge. As a specific example, a constant phase operator corresponds to a static phase bias, which gives rise to the standard supercurrent. A classical, time-dependent voltage bias $V(t)$ induces a dynamic phase $\hat{\phi}(t) = \int_{t_s}^t dt' eV(t')/\hbar$, which describes the ac Josephson effect in the case of a constant voltage, see Eq. (A27a), and gives rise to Shapiro steps when the drive is harmonic. In general, the dynamics of the phase operator is captured by a Hamiltonian $\hat{H}_{\mathrm{env}}$. Then, the total Hamiltonian is given by [12]

$$\hat{H} = \hat{H}_{\mathrm{cond}} + \hat{H}_{\mathrm{env}} + \hat{H}_{\mathrm{int}}. \tag{A1b}$$

2. Cumulant-generating functional

The statistics of the current $\hat{I}_{\rm H}(t)$ is fully encoded in the partition functional [16,21–24]

$$\mathcal{Z}[\chi] = \left\langle \tilde{\mathbb{T}}\left[e^{\frac{i}{e}\int_{t_s}^{\infty} dt\,\chi^{-}(t)\hat{I}_{\rm H}(t)}\right]\mathbb{T}\left[e^{-\frac{i}{e}\int_{t_s}^{\infty} dt\,\chi^{+}(t)\hat{I}_{\rm H}(t)}\right]\right\rangle, \tag{A2}$$

where $\mathbb{T}$ and $\tilde{\mathbb{T}}$ denote the time-ordering and anti-time-ordering operators, respectively. The functions $\chi^{+}(t)$ and $\chi^{-}(t)$ are the forward and backward components of the counting field defined on the Keldysh contour $C = C^{+} + C^{-}$, which runs from t_s to infinity and back to t_s. The subscript H indicates that the operator evolves in the Heisenberg picture, i.e., according to the Hamiltonian given in Eq. (A1b). The average $\langle\cdot\rangle$ is taken with respect to the initial density matrix $\hat{\varrho} = \hat{\varrho}_{\rm cond} \otimes \hat{\varrho}_{\rm env}$, which is assumed to be separable. Taking the logarithm of the partition functional results in the CGF $\mathcal{S}[\chi] = \log(\mathcal{Z}[\chi])$. Time-ordered current correlations can be obtained by functionally differentiating the moment-generating functional with respect to the counting field.

The average current and the noise are obtained by

$$\langle \hat{I}_{\rm H}(t)\rangle = ie\frac{\delta\mathcal{S}[\chi]}{\delta\chi^{q}(t)}\bigg|_{\chi=0} \tag{A3a}$$

$$\langle\{\Delta\hat{I}_{\rm H}(t), \Delta\hat{I}_{\rm H}(t')\}\rangle = -e^2\frac{\delta^2\mathcal{S}[\chi]}{\delta\chi^{q}(t)\delta\chi^{q}(t')}\bigg|_{\chi=0}, \tag{A3b}$$

with the quantum field $\chi^{q}(t) = \chi^{+}(t) - \chi^{-}(t)$, $\{\cdot,\cdot\}$ the anticommutator and $\Delta\hat{I}_{\rm H}(t) = \hat{I}_{\rm H}(t) - \langle\hat{I}_{\rm H}(t)\rangle$ the difference to the mean [15,25].

The central idea is to express the partition functional of Eq. (A2) in terms of the known partition functional for an isolated tunnel junction [23,24]. For this purpose, we transition to the interaction picture to decouple the dynamics of the junction and the environment. An operator $\hat{O}_{\rm H}(t)$ in the Heisenberg picture is related to the operator in the interaction picture $\hat{O}_{\rm I}(t)$ by

$$\hat{O}_{\rm H}(t) = \hat{U}_{\rm int}^{\dagger}(t,t_s)\hat{O}_{\rm I}(t)\hat{U}_{\rm int}(t,t_s), \tag{A4a}$$

where

$$\hat{U}_{\rm int}(t,t_s) = \mathbb{T}\exp\left(-\frac{i}{\hbar}\int_{t_s}^{t}\hat{H}_{\rm int}^{\rm I}(t')dt'\right) \tag{A4b}$$

is the interaction-picture evolution operator, and

$$\hat{H}_{\rm int}^{\rm I}(t) = \frac{\hbar}{e}\hat{\phi}_{\rm I}(t)\hat{I}_{\rm I}(t), \tag{A4c}$$

with the subscript I indicating operators in the interaction picture. The operator $\hat{\phi}_{\rm I}(t)$ evolves under the Hamiltonian $\hat{H}_{\rm env}$, while $\hat{I}_{\rm I}(t)$ evolves under $\hat{H}_{\rm cond}$. To simplify the notation, we promote the time variable to the full Keldysh contour C, and introduce the contour-ordering operator $\mathbb{T}_{\rm C}$, the contour evolution operator $\hat{U}_{\rm int}^{\rm C} = \mathbb{T}_{\rm C}\exp(-\frac{i}{\hbar}\int_{\rm C} dt\hat{H}_{\rm int}^{\rm I}(t))$, and a unified counting field $\chi(t)$, which equals $\chi^{+}(t)$ on the forward branch and $\chi^{-}(t)$ on the backward branch of the contour. The partition functional transforms to

$$\begin{aligned}
\mathcal{Z}[\chi] &= \sum_{n=0}^{\infty}\frac{(-i)^n}{n!}\int_{\rm C}dt_1\ldots\int_{\rm C}dt_n\langle\mathbb{T}_{\rm C}[\chi(t_1)\hat{I}_{\rm H}(t_1)\ldots\chi(t_n)\hat{I}_{\rm H}(t_n)]\rangle\\
&= 1 + \sum_{n=1}^{\infty}\frac{(-i)^n}{n!}\int_{\rm C}dt_1\ldots\int_{\rm C}dt_n\langle\mathbb{T}_{\rm C}[\hat{U}_{\rm int}(t_s,t_1)\chi(t_1)\hat{I}_{\rm I}(t_1)\ldots\hat{U}_{\rm int}(t_{n-1},t_n)\chi(t_n)\hat{I}_{\rm I}(t_n)\hat{U}_{\rm int}(t_n,t_s)]\rangle\\
&= 1 + \sum_{n=1}^{\infty}\frac{(-i)^n}{n!}\int_{\rm C}dt_1\ldots\int_{\rm C}dt_n\left\langle\mathbb{T}_{\rm C}\left[\hat{U}_{\rm int}^{\rm C}\chi(t_1)\hat{I}_{\rm I}(t_1)\ldots\chi(t_n)\hat{I}_{\rm I}(t_n)\right]\right\rangle + \left\langle\mathbb{T}_{\rm C}\hat{U}_{\rm int}^{\rm C}\right\rangle - \left\langle\mathbb{T}_{\rm C}\hat{U}_{\rm int}^{\rm C}\right\rangle\\
&= 1 + \left\langle\mathbb{T}_{\rm C}\exp\left(-\frac{i}{e}\int_{\rm C}[\chi(t)+\hat{\phi}_{\rm I}(t)]\hat{I}_{\rm I}(t)dt\right)\right\rangle - \left\langle\mathbb{T}_{\rm C}\hat{U}_{\rm int}^{\rm C}\right\rangle\\
&= 1 + \sum_{m=0}^{\infty}\frac{g^m}{m!}\int_{\rm C}dt_1\ldots\int_{\rm C}dt_m\left[\frac{\delta^m\mathcal{Z}_0[\chi]}{\delta\chi(t_1)\ldots\delta\chi(t_m)} - \frac{\delta^m\mathcal{Z}_0[\chi]}{\delta\chi(t_1)\ldots\delta\chi(t_m)}\bigg|_{\chi=0}\right]\langle\mathbb{T}_{\rm C}[\hat{\phi}_{\rm I}(t_1)\ldots\hat{\phi}_{\rm I}(t_m)]\rangle_{\rm env},
\end{aligned} \tag{A5}$$

with the partition functional $\mathcal{Z}_0[\chi]$ of the isolated tunnel junction, and $\langle\cdot\rangle_{\rm env}$ the average with respect to the environment's density matrix $\hat{\rho}_{\rm env}$. The final line is obtained by expanding $\hat{U}_{\rm int}^{\rm C}$ and exploitation of the defining property of the partition functional. The term $\langle\mathbb{T}_{\rm C}\hat{U}_{\rm int}^{\rm C}\rangle$ ensures proper normalization of the partition functional, such that $\mathcal{Z}[0] = 1$. The partition functional formally resembles a functional Taylor expansion of $1 + \langle\mathbb{T}_{\rm C}[\mathcal{Z}_0[\chi+\delta\chi] - \mathcal{Z}_0[\delta\chi]]\rangle_{\rm env}$, with a displacement $\delta\chi(t) = \hat{\phi}_{\rm I}(t)$.

The CGF (or Keldysh action) for a general multiterminal and time-dependent scatterer was derived by Snyman and Nazarov [23,26]. In a two-terminal device with an energy-independent scattering matrix, the CGF is given by [23,24,26,27]

$$\mathcal{S}_0[\chi] = \frac{1}{4}\sum_{n}\mathrm{Tr}\ln\left(1 + \frac{T_n}{4}(\{\check{G}_1(\chi),\check{G}_2\} - 2)\right), \tag{A6}$$

where $\check{G}_1(\chi)$ is the counting-field-dependent Green's function of terminal 1, $\check{G}_2$ is the corresponding Green's function of terminal 2, and T_n are transmission eigenvalues. The Green's functions are treated as operators in time, Keldysh,

Nambu, spin, and channel space, and Tr represents the trace over all these degrees of freedom. Operator multiplication involves integration over the time variable, while the remaining spaces (Keldysh, Nambu, spin, and channel) entail summation over discrete indices. For example, $[\check{G}_1\check{G}_2](t,t'') \equiv \int_C dt' \check{G}_1(t,t')\check{G}_2(t',t'')$. Note that the the Green's functions $\check{G}_{1,2}$ are defined with a third Pauli matrix in Keldysh space to ensure normalization $\check{G}_{1,2}\check{G}_{1,2} = \check{1}$, but therefore the Keldysh $-+/--$ components correspond to the negative of the greater/antitime ordered Green's function. The counting-field is incorporated in terminal 1 by [16,22,24]

$$\check{G}_1(\chi,t,t') = e^{-i\chi(t)\hat{\sigma}_3}\check{G}_1(t,t')e^{i\chi(t')\hat{\sigma}_3}, \tag{A7}$$

with $\hat{\sigma}_3$ the third Pauli-matrix in Nambu space.

We calculate the CGF $\mathcal{S}[\chi]$ in the tunnel limit and therefore retain only terms that are first order in the tunnel conductance $G_T = e^2\sum_n T_n/(\pi\hbar)$. In principle, higher-order terms can be obtained by expanding the CGF to the desired order in the tunnel conductance G_T, although the expressions become increasingly cumbersome. After tracing out the Keldysh and Nambu structure, we obtain

$$\mathcal{S}[\chi] = \frac{G_T\pi\hbar}{8e^2}\iint_{t_s}^{\infty} dtdt' \sum_{\substack{\nu,\nu'=\pm\\ \mu,\mu'=\pm}} (e^{-i\mu\chi^{\nu}(t)+i\mu'\chi^{\nu'}(t')} - 1)G_{\rm env}^{\nu\nu'\mu\mu'}(t,t')\mathrm{Tr}\tilde{G}_1^{\nu\nu'\mu\mu'}(t,t')\tilde{G}_2^{\nu'\nu\mu'\mu}(t',t), \tag{A8a}$$

with $\tilde{G}_j^{\nu\nu'\mu\mu'}$, $j=1,2$ a matrix in spin space, and $\mathrm{Tr}\{\cdot\}$ the trace in spin space. The indices ν, ν' refer to the Keldysh structure, with $\nu=+$ labeling the forward contour and $\nu=-$ the backward contour. The indices μ, μ' correspond to the Nambu structure, where $\mu=+$ denotes the particle component and $\mu=-$ the hole component. The Green's functions $\check{G}_j$ are assumed to have a trivial spin structure, corresponding to the identity matrix. The environmental Green's functions are

$$G_{\rm env}^{++\mu\mu'}(t,t') = \langle \mathbb{T}\, e^{-i\mu\hat{\phi}_1(t)}e^{i\mu'\hat{\phi}_1(t')}\rangle_{\rm env}, \tag{A8b}$$

$$G_{\rm env}^{--\mu\mu'}(t,t') = \langle \tilde{\mathbb{T}}\, e^{-i\mu\hat{\phi}_1(t)}e^{i\mu'\hat{\phi}_1(t')}\rangle_{\rm env}, \tag{A8c}$$

$$G_{\rm env}^{+-\mu\mu'}(t,t') = \langle e^{i\mu'\hat{\phi}_1(t')}e^{-i\mu\hat{\phi}_1(t)}\rangle_{\rm env}, \tag{A8d}$$

$$G_{\rm env}^{-+\mu\mu'}(t,t') = \langle e^{-i\mu\hat{\phi}_1(t)}e^{i\mu'\hat{\phi}_1(t')}\rangle_{\rm env}. \tag{A8e}$$

3. Full counting statistics

The FCSs are obtained using the fields $\chi^{\pm}(t) = \pm(1-\Theta(t-t_e))\chi/2$, where χ is the counting variable and the measurement interval runs from t_s to t_e. The CGF, derived from Eq. (A8a), is given by

$$\mathcal{S}(\chi) = (e^{-i\chi}-1)N_{21} + (e^{i\chi}-1)N_{12}. \tag{A9}$$

For a normal-metal junction, N_{21} and N_{12} represent the number of charges transferred from terminal 1 to terminal 2, and from terminal 2 to terminal 1, respectively. The charge transfer statistics follow a generalized Poisson distribution, as expected for transport through a tunnel junction [22]. Accounting for higher-order terms in the conductance G_T causes deviations from Poissonian statistics, whereas in the absence of a quantum environment, the resulting full counting statistics is multinomial [13–15,17,27–30]. A superconducting tunnel junction can exhibit negative values for N_{21} and N_{12}, thereby undermining the interpretation of the FCS as a probability distribution. However, the FCSs are observable when the dynamics of an idealized measurement device is taken into account [27]. Quasiparticles and Cooper pairs contribute to charge transfer such that

$$N_{jk} = N_{jk}^{\rm QP} + N_{jk}^{\rm CP}, \tag{A10a}$$

with the individual contributions

$$N_{21}^{\rm QP} = \frac{1}{e}\int_{-\infty}^{\infty} dE \sum_{\substack{\nu,\nu'=\pm\\ \nu\neq\nu'}} \overline{G}_{\rm env}^{\nu\nu'\nu\nu}(E)\Gamma^{\nu\nu'\nu\nu}(E), \tag{A10b}$$

$$N_{21}^{\rm CP} = \frac{1}{e}\int_{-\infty}^{\infty} dE \sum_{\substack{\nu,\nu'=\pm\\ \nu\neq\nu'}} \overline{G}_{\rm env}^{\nu\nu\nu\nu'}(E)\Gamma^{\nu\nu\nu\nu'}(E), \tag{A10c}$$

$$N_{12}^{\rm QP} = \frac{1}{e}\int_{-\infty}^{\infty} dE \sum_{\substack{\nu,\nu'=\pm\\ \nu\neq\nu'}} \overline{G}_{\rm env}^{\nu'\nu\nu\nu}(E)\Gamma^{\nu'\nu\nu\nu}(E), \tag{A10d}$$

$$N_{12}^{\rm CP} = \frac{1}{e}\int_{-\infty}^{\infty} dE \sum_{\substack{\nu,\nu'=\pm\\ \nu\neq\nu'}} \overline{G}_{\rm env}^{\nu\nu\nu'\nu}(E)\Gamma^{\nu\nu\nu'\nu}(E), \tag{A10e}$$

where

$$\overline{G}_{\rm env}^{\nu\nu'\mu\mu'}(E) = \iint_{t_s}^{t_e}\frac{dtdt'}{4\pi\hbar}e^{iE(t-t')/\hbar}G_{\rm env}^{\nu\nu'\mu\mu'}(t,t') \tag{A10f}$$

is the time-averaged environmental Green's function. In the absence of an electromagnetic environment, the tunneling rates are

$$\Gamma^{\nu\nu'\mu\mu'}(E) = \frac{G_T}{8e}\int_{-\infty}^{\infty} d\epsilon \mathrm{Tr}\tilde{G}_1^{\nu\nu'\mu\mu'}(\epsilon-E)\tilde{G}_2^{\nu'\nu\mu'\mu}(\epsilon), \tag{A10g}$$

with the energy domain representation $G_j^{\nu\nu'\mu\mu'}(E) = \int_{-\infty}^{\infty} e^{iE\tau/\hbar}d\tau G_j^{\nu\nu'\mu\mu'}(\tau)$, where $\tau = t-t'$. Here, the terminals are assumed to be in thermal equilibrium, which implies time-translation invariance of the Green's functions, i.e., $G_j^{\nu\nu'\mu\mu'}(t,t') = G_j^{\nu\nu'\mu\mu'}(t-t')$. The Green's function in Keldysh space takes the form

$$\begin{aligned}\check{G}_j &= \begin{pmatrix}\hat{G}_j^{++} & \hat{G}_j^{+-}\\ \hat{G}_j^{-+} & \hat{G}_j^{--}\end{pmatrix}\\ &= \frac{1}{2}\begin{pmatrix}\hat{G}_j^a+\hat{G}_j^r+\hat{G}_j^k & \hat{G}_j^a-\hat{G}_j^r+\hat{G}_j^k\\ \hat{G}_j^a-\hat{G}_j^r-\hat{G}_j^k & \hat{G}_j^a+\hat{G}_j^r-\hat{G}_j^k\end{pmatrix},\end{aligned} \tag{A11}$$

with the retarded/advanced $\hat{G}_j^{r/a}(E)$ component, and the Keldysh component $\hat{G}_j^k = (\hat{G}_j^r(E) - \hat{G}_j^a(E))(1 - 2f_j(E))$, where $f_j(E) = (1 + e^{(E-\tilde{\mu}_j)/(k_B T_j)})^{-1}$ is the Fermi-Dirac distribution. The Fermi-Dirac distribution is determined by the temperature T_j, and the chemical potential $\tilde{\mu}_j$ of the corresponding terminal.

A pure voltage bias V results in the environmental Green's functions

$$\overline{G}_{\rm env}^{\nu\nu'\mu\mu'}(E) = \frac{t_0 \delta(E - \mu' eV) e^{i\phi_0(\mu'-\mu)/2}}{2} \times \begin{cases} 1 & \mu = \mu' \\ \frac{\exp(i\mu'\omega_J t_0) - 1}{i\mu'\omega_J t_0} & \mu \neq \mu' \end{cases}, \tag{A12}$$

with Josephson frequency $\omega_J = 2eV/\hbar$, the superconducting phase difference ϕ_0, and the length of the measurement interval $t_0 = t_e - t_s$. Here, we assume that the measurement interval is large, such that $\omega_J t_0 \gg 1$. The components $N_{jk}^{\rm CP}$ oscillate at ω_J, reflecting the ac Josephson effect. As expected for transport under voltage bias [22], the number of transferred quasiparticles is given by the tunneling rates times the measurement interval.

4. Tunnel current

The tunnel current $I(t) = \langle \hat{I}_{\rm H}(t) \rangle$ is obtained by functionally differentiating the CGF with respect to the counting field, see Eq. (A3a). This yields the expression

$$I(t) = \sum_{\substack{\nu \neq \nu' = \pm \\ \mu\mu' = \pm}} \int_{-\infty}^{\infty} dE\, P^{\nu\nu'\mu\mu'}(t, E) \Gamma^{\nu\nu'\mu\mu'}(E), \tag{A13}$$

with the generalized P function

$$P^{\nu\nu'\mu\mu'}(t, E) = \int_0^{t-t_s} \frac{d\tau}{2\pi\hbar} \big(\mu\nu e^{iE\tau/\hbar} G_{\rm env}^{\nu\nu'\mu\mu'}(t, t-\tau) - \mu'\nu' e^{-iE\tau/\hbar} G_{\rm env}^{\nu\nu'\mu\mu'}(t-\tau, t) \big). \tag{A14}$$

We employed the identities relating time-ordered and anti-time-ordered Green's functions to the lesser and greater components in order to eliminate the $++/--$ contributions.

5. Normal conducting tunnel junction

In this subsection, we examine a tunnel junction between two normal conductors interacting with an environment. The retarded/advanced Green's function of a normal lead is

$$\hat{G}^{r/a}(E) = \pm \hat{\tau}_0 \otimes \hat{\sigma}_3, \tag{A15}$$

with $\hat{\tau}_0$ the zeroth Pauli matrix in spin space, and $\hat{\sigma}_3$ the third Pauli matrix in Nambu space. The rates $\Gamma^{\nu\nu'\mu\mu'}$ with $\mu \neq \mu'$ vanish. The remaining nonzero rates simplify to $\Gamma^{\nu\nu'\mu\mu}(E) = \Gamma(\nu' E)$, for $\nu \neq \nu'$, and $\Gamma(E)$ represents the tunneling rate of the uncoupled junction:

$$\Gamma(E) = \frac{G_T}{e} \int_{-\infty}^{\infty} d\epsilon [1 - f(\epsilon - E)] f(\epsilon) = \frac{G_T}{e} \frac{E}{1 - e^{-E/(k_B T)}}, \tag{A16}$$

where we assume equal temperatures $T_1 = T_2 = T$ and a Fermi-Dirac distribution $f(E)$ with zero chemical potential. The average current reduces to

$$I(t) = \sum_{\nu=\pm} \nu \int_{-\infty}^{\infty} dE\, P^{\nu}(t, E) \Gamma(E), \tag{A17}$$

with the P functions

$$P^{\nu}(t, E) = \int_0^{\infty} \frac{d\tau}{\pi\hbar} {\rm Re}(e^{iE\tau/\hbar} \langle e^{i\nu\hat{\phi}_1(t)} e^{-i\nu\hat{\phi}_1(t-\tau)} \rangle), \tag{A18}$$

where, for brevity, $\langle \cdot \rangle \equiv \langle \cdot \rangle_{\rm env}$. We consider the perturbation to have been switched on in the distant past, and took the limit $t_s \to -\infty$. Therefore, we recover the standard expressions of dynamical Coulomb blockade physics [18,19], and the formula derived in Ref. [11] for a nonequilibrium environment.

6. Superconducting tunnel junction

We turn to the case of a superconducting tunnel junction coupled to an environment, examining how the environment impacts both the quasiparticle and Cooper pair tunneling currents. The superconducting Green's function acquires a nontrivial matrix structure in Nambu space, reflecting the intrinsic particle-hole coherence characteristic of the superconducting state. The retarded and advanced Green's functions are given by

$$\hat{G}_j^{r/a} = \hat{\tau}_0 \otimes \frac{-i}{\sqrt{\Delta_j^2 - (E \pm i\eta)^2}} \begin{pmatrix} (E \pm i\eta) & \Delta_j e^{i\phi_j} \\ -\Delta_j e^{-i\phi_j} & -(E \pm i\eta) \end{pmatrix}, \tag{A19}$$

with Δ_j the superconducting gap, ϕ_j the superconducting phase, and the broadening parameter η, which tends to zero, but can be kept finite to describe inelastic processes, which broaden the electronic states. The superconducting phases ϕ_j are set to zero in the following, as they are already accounted for in $\hat{\phi}_1(t)$. The normalization condition requires $\hat{G}^{r/a}\hat{G}^{r/a} = \hat{1}$, where $\hat{1}$ is the identity in spin-Nambu space.

The quasiparticle current is associated with the diagonal components in Nambu space, corresponding to terms with $\mu = \mu'$. The corresponding rates are $\Gamma^{\nu\nu'\mu\mu}(E) = \Gamma_{\rm QP}(\nu' E)$, $\nu \neq \nu'$, with

$$\Gamma_{\rm QP}(E) = \frac{G_T}{e} \int_{-\infty}^{\infty} d\epsilon\, \varrho_1(\epsilon - E) \varrho_2(\epsilon) [1 - f(\epsilon - E)] f(\epsilon), \tag{A20a}$$

and the superconducting density of states

$$\varrho_j(E) = {\rm Re} \left(\frac{-i(E + i\eta)}{\sqrt{\Delta_j^2 - (E + i\eta)^2}} \right). \tag{A20b}$$

The resulting quasiparticle current,

$$I(t) = \sum_{\nu=\pm} \nu \int_{-\infty}^{\infty} dE\, P^{\nu}(t, E) \Gamma_{\rm QP}(E), \tag{A21}$$

exhibits the same structure as the electron current discussed in the previous section and involves the same P function defined in Eq. (3a). The only difference lies in the bare quasiparticle

tunneling rate, which additionally incorporates the superconducting densities of states.

The Cooper pair current originates from the anomalous (off-diagonal) components of the Green's functions, corresponding to $\mu \neq \mu'$, and gives rise to transition rates of the form $\Gamma^{\nu\nu'\mu\mu'}(E) = -\Gamma_{\rm CP}(\nu' E)$, for $\nu \neq \nu'$ and $\mu \neq \mu'$. The Cooper pair tunneling rate $\Gamma_{\rm CP}(E)$ is given by

$$\Gamma_{\rm CP}(E) = \frac{G_{\rm T}}{e}\int_{-\infty}^{\infty} d\epsilon\, \varsigma_1(\epsilon - E)\varsigma_2(\epsilon)[1 - f(\epsilon - E)]f(\epsilon), \tag{A22a}$$

with the pair densities

$$\varsigma_j(E) = \mathrm{Re}\left(\frac{i\Delta_j}{\sqrt{\Delta_j^2 - (E + i\eta)^2}}\right). \tag{A22b}$$

Cooper pair tunneling leads to the contribution

$$I_{\rm CP}(t) = \sum_{\nu=\pm} \nu \int_{-\infty}^{\infty} dE\, C^{\nu}(t, E)\Gamma_{\rm CP}(E), \tag{A23}$$

with a correlation function

$$C^{\nu}(t, E) = \int_0^{\infty} \frac{d\tau}{\pi\hbar}\,\mathrm{Re}(e^{iE\tau/\hbar}\langle e^{-i\nu\hat{\phi}_1(t)}e^{-i\nu\hat{\phi}_1(t-\tau)}\rangle). \tag{A24}$$

A dc voltage V and a superconducting phase shift applied additionally to the tunnel junction leads to a dynamical phase $\varphi_{dc}(t) = eVt/\hbar + \phi_0/2$, and can be incorporated by $\hat{\phi}_1(t) = \hat{\varphi}_1(t) + \varphi_{dc}(t)$, where $\hat{\varphi}$ is the phase operator of the environment. Thus, the P and C functions are

$$P^{\nu}(t, E) = \int_0^{\infty} \frac{d\tau}{\pi\hbar}\,\mathrm{Re}(e^{i(E+\nu eV)\tau/\hbar}\langle e^{i\nu\hat{\varphi}_1(t)}e^{-i\nu\hat{\varphi}_1(t-\tau)}\rangle) \tag{A25a}$$

$$C^{\nu}(t, E) = \int_0^{\infty} \frac{d\tau}{\pi\hbar}\,\mathrm{Re}(e^{i(E+\nu eV)\tau/\hbar}e^{-i\nu\phi_0 - 2i\nu eVt/\hbar}\langle e^{-i\nu\hat{\varphi}_1(t)} \times e^{-i\nu\hat{\varphi}_1(t-\tau)}\rangle). \tag{A25b}$$

To our knowledge, the C function has not been discussed in the literature in this level of generality and constitutes the unique part of our work.

7. ac Josephson effect and Shapiro steps

A constant voltage bias represents the most basic example of an electromagnetic environment. The C function reduces to

$$C^{\nu}(t, E) = \cos(\phi_0 + 2eVt/\hbar)\delta(E + \nu eV) + \nu \sin(\phi_0 + 2eVt/\hbar)\frac{1}{\pi}\mathrm{P.V.}\left[\frac{1}{E + \nu eV}\right], \tag{A26}$$

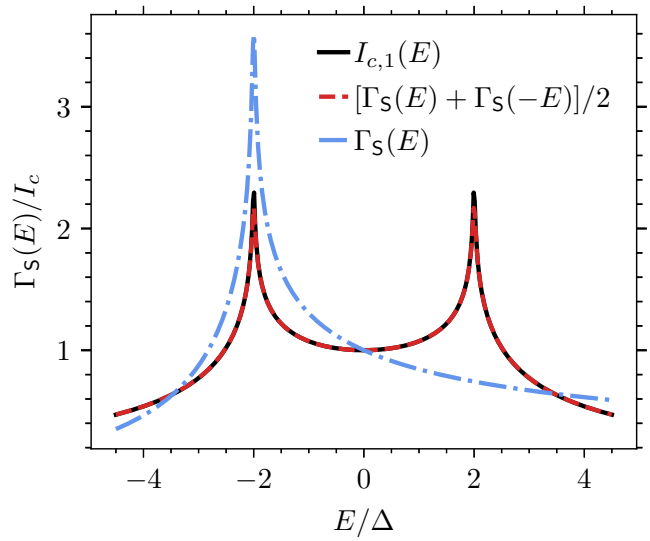

FIG. 8. Comparison between the rate $\Gamma_{\rm S}$ from Eq. (6c) of the main text and the critical current $I_{\rm c,1}$. The plot illustrates that the critical current is given by the symmetrized rate evaluated at $\pm eV$. Parameter: zero temperature, broadening $\eta = 5 \times 10^{-3}$.

with P.V. the principal value. The Cooper pair current is given by

$$I_{\rm CP}(t) = I_{\rm c,1}(V)\sin(\phi_0 + 2eVt/\hbar) + I_{\rm c,2}(V)\cos(\phi_0 + 2eVt/\hbar), \tag{A27a}$$

with the current amplitudes

$$I_{\rm c,1}(V) = \frac{G_{\rm T}}{\pi e}\mathrm{P.V.}\int\!\!\int_{-\infty}^{\infty} dE d\epsilon \frac{\varsigma_1(E)\varsigma_2(\epsilon)}{E - \epsilon - eV}[f(E) - f(\epsilon)] \tag{A27b}$$

$$I_{\rm c,2}(V) = \frac{G_{\rm T}}{e}\int_{-\infty}^{\infty} d\epsilon\,\varsigma_1(\epsilon - eV)\varsigma_2(\epsilon)[f(\epsilon - eV) - f(\epsilon)]. \tag{A27c}$$

We recover the well-known ac Josephson effect [1,31]. The rate $\Gamma_{\rm S}(E)$, as defined in the main text, is related to the critical current amplitude $I_{\rm c,1}(V)$ via the relation $I_{\rm c,1}(V) = [\Gamma_{\rm S}(eV) + \Gamma_{\rm S}(-eV)]/2$, as shown in Fig. 8.

An external microwave field incident at the tunnel junction is modeled by a voltage $V(t) = V_0\cos(\omega_0 t)$, where V_0 and ω_0 are the amplitude and angular frequency of the microwave drive, respectively. The time-dependent voltage induces a dynamical phase

$$\phi(t) = \frac{eV}{\hbar}t + a\sin(\omega_0 t), \tag{A28}$$

where V corresponds to the applied dc voltage and $a = eV_0/(\hbar\omega_0)$ to the strength of the drive. Therefore, the environmental phase $\hat{\phi}(t) = \phi(t)$ results in

$$C^{\nu}(t, E) = \sum_{n,l=-\infty}^{\infty} J_n(a)J_l(a)\Big(\cos(\phi_0 + \Omega_{nl}t) \times \delta(E + \nu eV + \nu l\hbar\omega_0) + \nu\sin(\phi_0 + \Omega_{nl}t) \times \frac{1}{\pi}\mathrm{P.V.}\left[\frac{1}{E + \nu eV + \nu l\hbar\omega_0}\right]\Big), \tag{A29}$$

with $\Omega_{nl} = 2eV/\hbar + (n+l)\omega_0$. We utilized the identity $\exp(iz\sin(\Theta)) = \sum_{l=-\infty}^{\infty} J_l(z)\exp(il\Theta)$, where $J_l(z)$ denotes the Bessel function of the first kind of order l. The resulting Cooper pair current

$$I_{\mathrm{CP}}(t) = \sum_{n,l=-\infty}^{\infty} J_n(a)J_l(a)[\mathrm{I}_{\mathrm{c},2}(eV + l\hbar\omega_0)\cos(\phi_0 + \Omega_{nl}t) + \mathrm{I}_{\mathrm{c},1}(eV + l\hbar\omega_0)\sin(\phi_0 + \Omega_{nl}t)] \tag{A30}$$

oscillates at harmonics of the driving frequency and is consistent with the results reported in Ref. [1]. The time-averaged Cooper pair current

$$\begin{aligned}\bar{I}_{\mathrm{CP}} &= \lim_{\tilde{T}\to\infty}\frac{1}{\tilde{T}}\int_{-\tilde{T}/2}^{\tilde{T}/2} I_{\mathrm{CP}}(t)dt \\ &= \sum_{m=-\infty}^{\infty}\delta_{eV,m\hbar\omega_0/2}\sum_{l=-\infty}^{\infty} J_{m-l}(a)J_l(a) \\ &\quad\times[\mathrm{I}_{\mathrm{c},1}(eV + l\hbar\omega_0)\sin(\phi_0) - \mathrm{I}_{\mathrm{c},2}(eV + l\hbar\omega_0)\cos(\phi_0)]\end{aligned} \tag{A31}$$

exhibits spikes at $eV = m\hbar\omega_0/2$ in the $I-V$ curve, with $\delta_{eV,m\hbar\omega_0/2} = 1$ for $eV = m\hbar\omega_0/2$, and $\delta_{eV,m\hbar\omega_0/2} = 0$ for $eV \neq m\hbar\omega_0/2$. These spikes correspond to Shapiro steps in a current-biased tunnel junction [1,4].

8. State preparation

We envisage a finite-time state preparation protocol that initializes the environment in a desired state [7], after which the average tunnel current is measured over a substantially longer time interval. The time-averaged current of interest is

$$\bar{I} \equiv \frac{1}{t_{\mathrm{e}} - t_{\mathrm{m}}}\int_{t_{\mathrm{m}}}^{t_{\mathrm{e}}} dt I(t) = \bar{I}_{\mathrm{in}} + \bar{I}_{\mathrm{prep}}, \tag{A32}$$

where the preparation takes place from time t_{s} up to t_{m}, at which point the measurement begins and continues until t_{e}. The current $\bar{I}_{\mathrm{in}}$ depends solely on the prepared state, while $\bar{I}_{\mathrm{prep}}$ depends on the preparation protocol. The integrals in $\bar{I}_{\mathrm{in}}$ run over times later than t_{m} such that the environmental correlator can be reformulated as

$$\begin{aligned}&\langle e^{i\nu\hat{\varphi}_{\mathrm{I}}(t)}e^{-i\nu'\hat{\varphi}_{\mathrm{I}}(t')}\rangle \\ &= \mathrm{Tr}\{U^\dagger(t,t_{\mathrm{s}})e^{i\nu\hat{\varphi}}U(t,t_{\mathrm{s}})U^\dagger(t',t_{\mathrm{s}})e^{-i\nu'\hat{\varphi}}U(t',t_{\mathrm{s}})\hat{\rho}_{\mathrm{env}}\} \\ &= \mathrm{Tr}\{U^\dagger(t,t_{\mathrm{m}})e^{i\nu\hat{\varphi}}U(t,t_{\mathrm{m}})U^\dagger(t',t_{\mathrm{m}})e^{-i\nu'\hat{\varphi}}U(t',t_{\mathrm{m}}) \\ &\quad\times U(t_{\mathrm{m}},t_{\mathrm{s}})\hat{\rho}_{\mathrm{env}}U^\dagger(t_{\mathrm{m}},t_{\mathrm{s}})\} \\ &= \mathrm{Tr}\{e^{i\nu\hat{\varphi}_{\mathrm{m}}(t)}e^{-i\nu'\hat{\varphi}_{\mathrm{m}}(t')}\hat{\rho}_{\mathrm{in}}\},\end{aligned} \tag{A33}$$

with $\hat{\rho}_{\mathrm{env}}$ is the initial density matrix at t_{s}, $\hat{\rho}_{\mathrm{in}}$ the initialized density matrix at t_{m}, and $U(t,t_{\mathrm{s}})$ the time-evolution operator of the environment. The average current $\bar{I}_{\mathrm{prep}}$ involves correlators of the form

$$\frac{1}{t_{\mathrm{e}} - t_{\mathrm{m}}}\int_0^{t_{\mathrm{e}}-t_{\mathrm{m}}} dt\int_0^{t_{\mathrm{m}}-t_{\mathrm{s}}}\frac{d\tau}{\pi\hbar}\mathrm{Re}(e^{iE(t+\tau)/\hbar} \times\langle e^{i\nu\hat{\varphi}_{\mathrm{I}}(t+t_{\mathrm{m}})}e^{-i\nu'\hat{\varphi}_{\mathrm{I}}(t_{\mathrm{m}}-\tau)}\rangle), \tag{A34}$$

and is sensitive to the time evolution of the environmental operator during the state preparation period. If, $\hat{H}\,|E_n\rangle = E_n\,|E_n\rangle$, with a discrete set of eigenvalues E_n and orthonormal eigenstates $|E_n\rangle$, then

$$\frac{1}{t_{\mathrm{e}} - t_{\mathrm{m}}}\int_0^{t_{\mathrm{e}}-t_{\mathrm{m}}} dt e^{iEt/\hbar}e^{i\nu\hat{\varphi}_{\mathrm{m}}(t)} = \sum_{n,m}\langle n|\,e^{i\nu\hat{\varphi}}\,|m\rangle \times|n\rangle\,\langle m|\,\frac{1}{t_{\mathrm{e}} - t_{\mathrm{m}}}\int_0^{t_{\mathrm{e}}-t_{\mathrm{m}}} dt e^{i(E+E_n-E_m)t/\hbar}. \tag{A35}$$

The time average leads to a factor

$$\begin{aligned}&\frac{1}{t_{\mathrm{e}} - t_{\mathrm{m}}}\int_0^{t_{\mathrm{e}}-t_{\mathrm{m}}} dt e^{i(E+E_n-E_m)t/\hbar} \\ &= \frac{\cos(\Omega(t_{\mathrm{e}} - t_{\mathrm{m}}))}{i\Omega(t_{\mathrm{e}} - t_{\mathrm{m}})} + \frac{\sin(\Omega(t_{\mathrm{e}} - t_{\mathrm{m}}))}{\Omega(t_{\mathrm{e}} - t_{\mathrm{m}})} \\ &\quad - \frac{1}{i\Omega(t_{\mathrm{e}} - t_{\mathrm{m}})}\xrightarrow[t_{\mathrm{e}}-t_{\mathrm{m}}\to\infty]{}\delta_{\Omega,0},\end{aligned} \tag{A36}$$

with $\Omega = (E + E_n - E_m)/\hbar$. In the limit of a large measurement window, this factor becomes nonzero only when $E + E_n - E_m = 0$. Therefore, the integrand in the energy integral over E is nonzero only on a set of measure zero, implying that $\bar{I}_{\mathrm{prep}} \to 0$ in the limit $t_{\mathrm{e}} - t_{\mathrm{m}} \to \infty$. Including a finite voltage bias merely shifts Ω, while the underlying reasoning remains unchanged. This demonstrates that the average current $\bar{I} = \bar{I}_{\mathrm{in}}$ depends on the initialized state as well as on the system's evolution during the measurement interval, and not on the preparation protocol.

9. Example states

The states examined in the main text are a Fock state superposition, a coherent state, and a squeezed vacuum state. Charge transport depends on these states through the density matrix $\rho_{n+jn} = \langle n+j|\,\hat{\rho}\,|n\rangle, n+j, n \in \mathbb{N}$; see Eqs. (13a) and (14b) of the main text. The Fock state superposition $|\psi_{01}\rangle = [|0\rangle + e^{i\theta_1}\,|1\rangle]/2$ possesses the density matrix element

$$\rho_{n+jn} = \frac{1}{2}\begin{cases}1 & n \leqslant 1 \text{ and } j = 0\\ e^{i\theta_1} & n = 0 \text{ and } j = 1\\ e^{-i\theta_1} & n = 1 \text{ and } j = -1.\end{cases} \tag{A37}$$

The Coherent state $|\alpha\rangle$ yields a density matrix element

$$\rho_{n+jn} = \frac{|\alpha|^{2n}\alpha^{*j}}{\sqrt{n!(n+j)!}}e^{-|\alpha|^2}, \tag{A38}$$

with $\alpha = |\alpha|e^{i\theta_2} \in \mathbb{C}$ the coherent parameter. A squeezed vacuum state $|\xi\rangle$, characterized by the squeezing parameter $\xi = re^{i\theta_3}$, with $0 \leqslant r < \infty, 0 \leqslant \theta < 2\pi$, is given by [32]

$$|\xi\rangle = \frac{1}{\sqrt{\cosh(r)}}\sum_{m=0}^{\infty}(-1)^m\frac{\sqrt{(2m!)}}{2^m m!} \times e^{im\theta_3}(\tanh(r))^m\,|2m\rangle\,. \tag{A39}$$

The density matrix elements reduce to

$$\varrho_{n+jn} = \begin{cases}B_{nj}e^{ij\theta_3/2}\frac{[\tanh(r)]^{n+j/2}}{\cosh(r)} & n, j \text{ even}\\ 0 & \text{otherwise},\end{cases} \tag{A40}$$

with $B_{nj} = (-1)^{j/2}\sqrt{(n+j)!n!}/(2^{n+j/2}((n+j)/2)!(n/2)!)$. The structure of the density matrix is directly reflected in the Cooper pair transport: For the Fock state, only the peaks at $j = -1, 0, 1$ appear; for the squeezed vacuum state, only even-j peaks are present; while the coherent state exhibits peaks at all j.

[1] A. Barone and G. Paterno, *Physics and Applications of the Josephson Effect* (John Wiley & Sons, New York, 1982).

[2] A. H. Dayem and R. J. Martin, Quantum interaction of microwave radiation with tunneling between superconductors, Phys. Rev. Lett. **8**, 246 (1962).

[3] P. K. Tien and J. P. Gordon, Multiphoton process observed in the interaction of microwave fields with the tunneling between superconductor films, Phys. Rev. **129**, 647 (1963).

[4] S. Shapiro, Josephson currents in superconducting tunneling: The effect of microwaves and other observations, Phys. Rev. Lett. **11**, 80 (1963).

[5] A. Blais, A. L. Grimsmo, S. M. Girvin, and A. Wallraff, Circuit quantum electrodynamics, Rev. Mod. Phys. **93**, 025005 (2021).

[6] A. A. Clerk, K. W. Lehnert, P. Bertet, J. R. Petta, and Y. Nakamura, Hybrid quantum systems with circuit quantum electrodynamics, Nat. Phys. **16**, 257 (2020).

[7] M. Hofheinz, H. Wang, M. Ansmann, R. C. Bialczak, E. Lucero, M. Neeley, A. D. O'connell, D. Sank, J. Wenner, J. M. Martinis, and A. N. Cleland, Synthesizing arbitrary quantum states in a superconducting resonator, Nature (London) **459**, 546 (2009).

[8] L. Bretheau, Ç. Ö. Girit, H. Pothier, D. Esteve, and C. Urbina, Exciting Andreev pairs in a superconducting atomic contact, Nature (London) **499**, 312 (2013).

[9] L. Bretheau, Ç. Girit, M. Houzet, H. Pothier, D. Esteve, and C. Urbina, Theory of microwave spectroscopy of Andreev bound states with a Josephson junction, Phys. Rev. B **90**, 134506 (2014).

[10] G. Aiello, M. Féchant, A. Morvan, J. Basset, M. Aprili, J. Gabelli, and J. Estève, Quantum bath engineering of a high impedance microwave mode through quasiparticle tunneling, Nat. Commun. **13**, 7146 (2022).

[11] J.-R. Souquet, M. J. Woolley, J. Gabelli, P. Simon, and A. A. Clerk, Photon-assisted tunneling with nonclassical light, Nat. Commun. **5**, 5562 (2014).

[12] Y. V. Nazarov, *Quantum Noise in Mesoscopic Physics*, NATO Science Series II: Mathematics, Physics and Chemistry (Springer Science & Business Media, Dordrecht, 2012), Vol. 97.

[13] M. Vanević, Y. V. Nazarov, and W. Belzig, Elementary events of electron transfer in a voltage-driven quantum point contact, Phys. Rev. Lett. **99**, 076601 (2007).

[14] M. Vanević, Y. V. Nazarov, and W. Belzig, Elementary charge-transfer processes in mesoscopic conductors, Phys. Rev. B **78**, 245308 (2008).

[15] M. Kindermann and Y. V. Nazarov, Interaction effects on counting statistics and the transmission distribution, Phys. Rev. Lett. **91**, 136802 (2003).

[16] M. Kindermann, Y. V. Nazarov, and C. W. J. Beenakker, Feedback of the electromagnetic environment on current and voltage fluctuations out of equilibrium, Phys. Rev. B **69**, 035336 (2004).

[17] J. Tobiska and Y. V. Nazarov, Inelastic interaction corrections and universal relations for full counting statistics in a quantum contact, Phys. Rev. B **72**, 235328 (2005).

[18] G.-L. Ingold and Y. V. Nazarov, Charge tunneling rates in ultrasmall junctions, in *Single Charge Tunneling: Coulomb Blockade Phenomena In Nanostructures*, edited by H. Grabert and M. H. Devoret (Springer US, Boston, MA, 1992), pp. 21–107.

[19] P. Joyez, Self-consistent dynamics of a Josephson junction in the presence of an arbitrary environment, Phys. Rev. Lett. **110**, 217003 (2013).

[20] H. Grabert, Dynamical Coulomb blockade of tunnel junctions driven by alternating voltages, Phys. Rev. B **92**, 245433 (2015).

[21] L. S. Levitov, H. Lee, and G. B. Lesovik, Electron counting statistics and coherent states of electric current, J. Math. Phys. **37**, 4845 (1996).

[22] W. Belzig, Full counting statistics of superconductor-normal-metal heterostructures, in *Quantum Noise in Mesoscopic Physics*, edited by Y. V. Nazarov (Springer, Netherlands, Dordrecht, 2003), pp. 463–496.

[23] I. Snyman and Y. V. Nazarov, Keldysh action of a multiterminal time-dependent scatterer, Phys. Rev. B **77**, 165118 (2008).

[24] Y. V. Nazarov, Full counting statistics and field theory, Ann. Phys. **519**, 720 (2007).

[25] Y. M. Blanter and M. Büttiker, Shot noise in mesoscopic conductors, Phys. Rep. **336**, 1 (2000).

[26] Y. V. Nazarov, Block-determinant formalism for an action of a multi-terminal scatterer, Physica E **74**, 561 (2015).

[27] W. Belzig and Y. V. Nazarov, Full counting statistics of electron transfer between superconductors, Phys. Rev. Lett. **87**, 197006 (2001).

[28] J. C. Cuevas and W. Belzig, Full counting statistics of multiple Andreev reflections, Phys. Rev. Lett. **91**, 187001 (2003).

[29] J. C. Cuevas and W. Belzig, Dc transport in superconducting point contacts: A full-counting-statistics view, Phys. Rev. B **70**, 214512 (2004).

[30] M. Hübler and W. Belzig, Full counting statistics of ultrafast quantum transport, Appl. Phys. Lett. **123**, 034006 (2023).

[31] B. D. Josephson, Possible new effects in superconductive tunnelling, Phys. Lett. **1**, 251 (1962).

[32] C. C. Gerry and P. L. Knight, *Introductory Quantum Optics* (Cambridge University Press, Cambridge, 2023).